Segmental Orientation Behavior of Poly(butylene terephthalate-*co*-tetramethylene oxide) upon Uniaxial Deformation

Han Sup Lee,* Nam Woong Lee, Kwang Hyun Paik and Dae Woo Ihm†

Department of Textile Engineering, INHA University, Inchon, Korea, and Cheil Synthetic Inc., Research and Development Center, Gi-heung, Korea

Received November 29, 1993; Revised Manuscript Received May 4, 1994®

ABSTRACT: The segmental orientation behavior of the thermoplastic elastomer [poly(butylene terephthalate-*co*-tetramethylene oxide)] has been studied with infrared dichroism and polarizing microscopy. The orientation of hard segments as well as soft segments has been determined as a function of draw ratio. The difference in the orientation behavior of soft and hard segments has been associated with the respective glass transition temperatures. It has been also established that annealing significantly affects the deformation behavior. The segmental orientation has been observed to be strongly affected by the addition of small amount of the asymmetric chain extender. These results indicate that the crystalline structure of the hard segment can be significantly perturbed by the heterogeneity of the chain extender. The birefringence observed using the polarizing microscopy as a function of draw ratio correlates well with the orientation functions of hard segments rather than those of soft segments. It is known that π electrons in the hard-segment structure affect the refractive index significantly. Thus chemical structure of each segment in phase-separated thermoplastic elastomer should be considered in order to properly interpret birefringence data.

Introduction

Elastomers are widely used in polymer industries. Historically, vulcanized natural rubbers have been used since their discovery in the 19th century. The elastic property of natural rubber, i.e. elongation up to several hundred percent with recovery of its initial state upon removal of the external stress, is remarkable. Application of elastomers ranges from tires of various types of vehicles to fibers, surface coating materials, external and internal structural materials of automobiles, industrial materials, sports equipments, and parts of various instruments.[1,2]

Elastomers are classified into two types: thermosetting and thermoplastic elastomers. The elastic properties of thermosetting elastomers can be obtained by the chemical cross-linking of linear polymers which prevents permanent deformation of the chains. Furthermore, since the chains are chemically cross-linked, the shapes of thermosetting elastomers are permanently set during manufacturing and cannot be altered.

The elastic properties of thermoplastic elastomers (TPE) is attributed to the physical cross-links resulting from the phase separation of the constituent components. Since the phase separation is thermoreversible, the shape and structure of the thermoplastic elastomers can be altered and the processing condition of TPE, compared with the thermosetting elastomers, is simple.[3]

Poly(ether ester) copolymers are segmented block copolymers consisting of hard and soft segment units. When poly(butylene terephthalate) (PBT) is used as hard segment, the copolymer exhibits good mechanical properties such as elasticity, toughness, abrasion resistance, and low-temperature flexibility. PBT-based thermoplastic elastomers are commercially produced worldwide and their application ranges from automobile parts and structural materials of sports equipments to industrial rollers and hoses.[4,5]

Due to the incompatibility between the two structural units, the poly(ether ester) copolymers undergo microphase separation resulting in crystalline hard domains and soft-segment-rich soft domains. The exact domain structure is affected by the various factors such as chemical structure of the soft segment, chemical composition of the two segments, molecular weight of each segment, sample preparation method, and mechanical and thermal history.[6-10] Since the polymers have complicated heterogeneous structures, the exact correlation between the structure and the mechanical properties has not been established.

The thermoplastic elastomers undergo various types of deformation in various applications. Since mechanical properties such as elasticity, toughness, modulus, and stretchability of this polymer are determined by the internal structures, it is necessary to establish the structure–property relationship well. The structural changes upon uniaxial deformation of segmented copolyesters have been characterized by various methods such as infrared dichroism,[11,12] wide-angle X-ray diffraction,[6] and light-scattering methods.[7,13] The segmental orientation behaviors have been studied mainly with the infrared spectroscopy.[12,14,15] It was found that the orientation behavior of each segment of the thermoplastic elastomers was quite different.

In this study, the orientation behavior of each segment as well as overall chains have been measured with the infrared dichroic method and polarizing microscopy. The similarity and difference between the two sets of results are interpreted in terms of the chemical structure differences between the two segments.

Experimental Section

1. **Materials.** Two copolymers used in this study were kindly supplied by the Cheil Synthetic Inc. (Gi-heung, Korea). The general physical data are shown in Table 1 and the chemical structure is shown in Figure 1. Esrel 1040M contains a small amount (about 4%) of aromatic chain extender in addition to the butanediol. The polymers were dissolved in chloroform solvent (2–3% w/v) initially. To obtain thin films for infrared spectroscopy and microscopy studies, glass slides were dipped in the polymer solution and dried under atmospheric conditions

* Author to whom all correspondence should be addressed.
† Cheil Synthetic Inc.
® Abstract published in *Advance ACS Abstracts*, June 1, 1994.

0024-9297/94/2227-4364$04.50/0

PBT-co-PTMO ('ESREL')

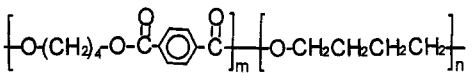

Hard Segment Soft Segment

Figure 1. Chemical structure of poly(butylene terephthalate-*co*-tetramethylene oxide), i.e., PBT-*co*-PTMO.

Table 1. Physical Data of Two Samples

sample	hard-segment content (%)	T_g (°C)	T_m (°C)
Esrel 1040M	43.8	-59.5	150
Esrel 1045	50.6	-59.3	192

for several hours followed by vacuum drying for several days at room temperature. In order to study the effect of annealing, the films on the slide were further annealed for 15 h at 5 °C below the melting temperature, i.e. $\Delta T = 5$ °C. Films for X-ray diffraction work were obtained by casting a film in a Teflon mold followed by the drying and annealing similar to the treatments used for spectroscopy and microscopy studies.

2. Infrared Spectroscopy. Infrared spectra were obtained with a Bruker Model IFS48 and a Nicolet Model 520P Fourier-transform infrared spectrometer. Spectral resolution was maintained at 2 cm^{-1}. The polarization of the incident infrared light was achieved with a gold wire polarizer on a KRS-5 substrate.

The films were stretched to a predefined level and maintained at that state for ~5 min before the infrared spectra were collected. Five min of relaxation time were found to be sufficiently long for samples to reach equilibrium. Two infrared spectra were collected successively with the polarizer parallel and perpendicular to the stretching direction. Infrared intensity of the selected bands was calculated based on band area after baseline correction had been made.

The dichroic ratio of each peak was obtained from the two ($A_\parallel$,$A_\perp$) infrared intensities with eq 1.

$$D = \frac{A_\parallel}{A_\perp} \tag{1}$$

The orientation function, f, of each peak was calculated from the dichroic value and eq 2,[16,17]

$$f = \frac{D_0 + 2}{D_0 - 1}\frac{D - 1}{D + 2} \tag{2}$$

where D_0 is the dichroic value of the perfectly oriented chain, which can be calculated from the transition dipole moment angle α and eq 3.

$$D_0 = 2\cot^2\alpha \tag{3}$$

3. Polarizing Microscopy. A small stretcher was constructed to stretch copolymer films on the sample stage of the polarizing microscope. The thickness change of the films upon stretching could not be expressed in terms of the Poisson ratio of the sample. Thus, the calibration curve for the thickness change upon deformation has been made by measuring the thickness at each draw ratio with a thickness measuring device, i.e., Elcometer 300.

The retardation value was obtained with Nikon Optiphot 2-pol Polarizing microscope. The miniature stretcher holding copolymer films was placed on the sample stage

BIREFRINGENCE by MICROSCOPY

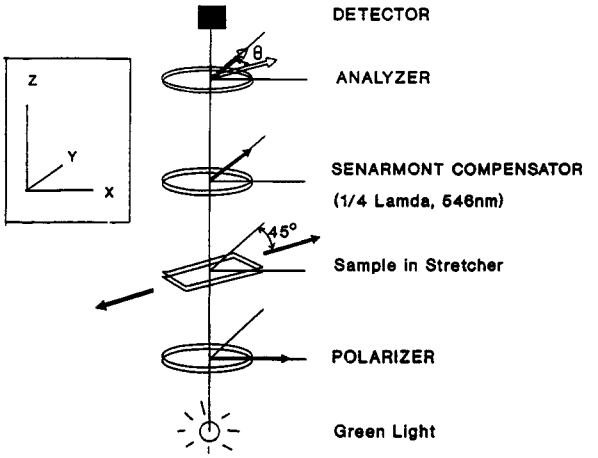

Figure 2. Schematic arrangement of the microscopic elements for the birefringence measurement.

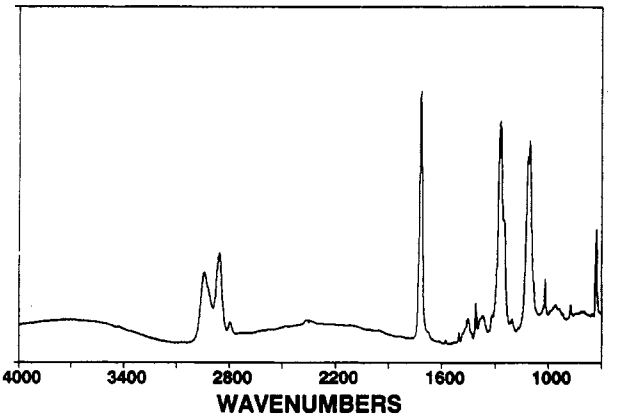

Figure 3. Infrared spectra of PBT-*co*-PTMO copolymer.

of the microscope with the stretching direction 45° to the polarizer direction. The monochromatic light (λ = 546 nm) was used. The Senarmont compensator was placed with its slow direction perpendicular to the polarizer direction. Similar to infrared experiments, the film was deformed and relaxed for about 5 min. Retardation, R, was calculated from the analyzer angle, θ, and eq 4,[18]

$$R = \frac{\theta}{\pi}\lambda \tag{4}$$

where θ is the analyzer angle at which the light intensity passing through the analyzer is the minimum. The initial direction (θ = 0) of the analyzer is perpendicular to the polarizer. The direction and placement of each component used are shown schematically in Figure 2.

The birefringence was calculated with the initial sample thickness, thickness calibration curve made previously, retardation value (R), and eq 5,

$$\Delta n = \frac{R}{d} \tag{5}$$

where d is the sample thickness at the corresponding state.

Results and Discussion

1. Infrared Dichroism Analysis. The infrared spectrum of poly(butylene terephthalate-*co*-tetramethylene oxide) (PBT-*co*-PTMO) is shown in Figure 3. For the peak assignment, the infrared spectra of pure hard as well as soft segments are shown in Figure 4. By comparing

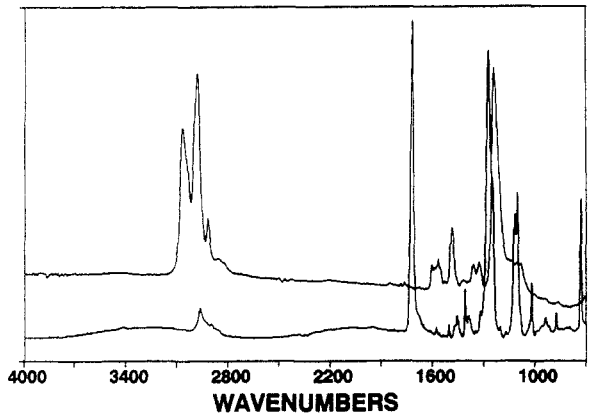

Figure 4. Infrared spectra of PBT and PTMO homopolymers.

Table 2. Assignment and Transition Dipole Moment Angle of Selected Infrared Peaks

wavenumbers	assignment[a]	α, deg
2945	C—H asymmetric stretching, mainly SS	90
2853	C—H symmetric stretching, mainly SS	90
1717	C=O stretching, HS	78
1112	C—O stretching, HS and SS	0
730	ring C—H out of plane bending, HS	90

[a] HS, hard segment; SS, soft segment.

the two sets of data, most of the peaks in Figure 3 can be assigned (Table 2).

Referring to the chemical structure in Figure 1, it is to be noted that the hard segment (HS) contains characteristic carbonyl and aromatic groups, whereas the soft segment contains a large amount of CH_2 and ether functional groups. Since the peaks at 1717 and 730 cm^{-1} are assignable to the hard segments, the orientational behavior of hard segments can be inferred from these infrared peaks. No infrared active vibrations assignable to soft segments can be found. However, it is obvious from Figure 4 that the C–H stretching peaks at 2945 and 2853 cm^{-1} are mostly due to the soft segments. The intensity of those peaks assignable to the hard segment, compared with that of soft segment, is relatively low. The shape of those peaks in Figure 3 also resembles that of the soft segment. All these results seem to indicate that the intensity of the C–H stretching peaks of copolymers is mainly due to the soft segments. In this study, the orientational behavior of the soft segments is estimated from the C–H stretching peaks. The error in assuming that the C–H stretching peaks are due to the soft segments appears to be negligible.

The infrared spectra of the Esrel 1040M polymer with two different polarizations at a 500% strain are shown in Figure 5. The dichroic behavior of the many peaks is obvious. It is to be noted that the dichroic behavior at 1717 and 730 cm^{-1} is stronger than that of C–H stretching peak. This seems to indicate qualitatively that the hard-segment orientation is greater than soft-segment orientation.

In Figure 6, the orientation functions of the hard and soft segment of the Esrel 1040M polymer are shown as a function of draw ratio. The transition dipole moment angles, α, of each peak used to calculate the orientation function are included in Table 2.[19,20] The data for annealed samples are also included in the figure. For the unannealed samples, the orientation function of soft segment gradually increases with the draw ratio (DR). However, hard segments orient abruptly at low draw ratio (up to DR = 4) and approaches the maximum value when drawn further. At DR = 6, for example, the orientation function of soft

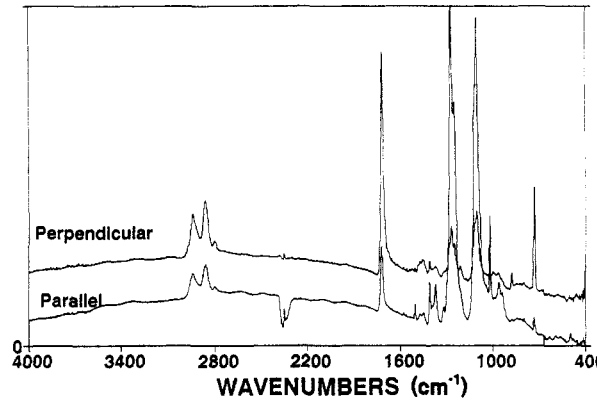

Figure 5. Infrared spectra of Esrel 1040M polymer obtained with two polarizer directions at a 500% strain.

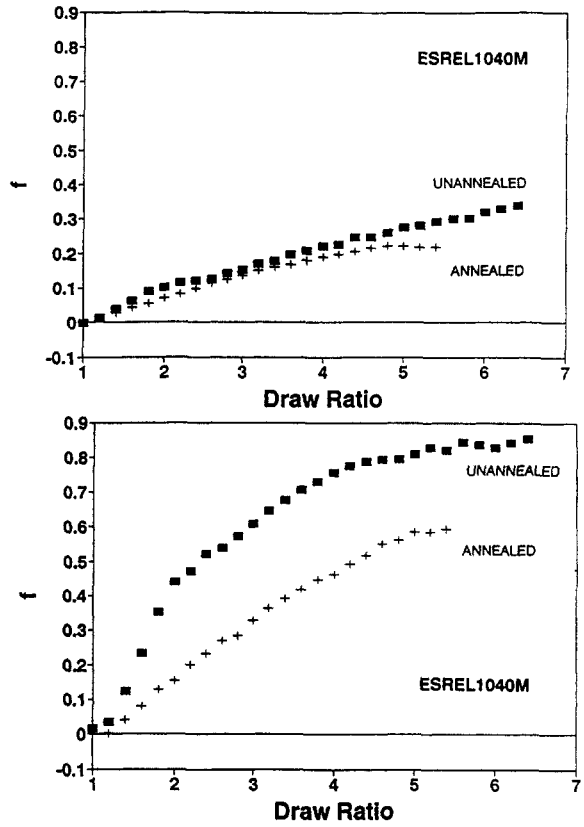

Figure 6. Orientation function of Esrel 1040M as a function of draw ratio: (a, top) C–H stretching, (b, bottom) aromatic C–H bending.

segment is about 0.30 compared with 0.83 of aromatic C–H stretching peaks. The effect of annealing on the orientation function is distinctive. Even though soft-segment orientation is negligibly affected by the annealing, the hard segment shows greatly diminished orientation upon annealing. This fact will be discussed further.

In Figure 7, orientation behaviors of both segments in Esrel 1045 polymer are shown. The orientation function of the soft segment (Figure 7a) is similar to that in Figure 6a. However, the hard segments of Esrel 1045 develop orientation quite differently from those of Esrel 1040M. The orientation function decreases initially for DR < 1.5 followed by the gradual increase. The value of orientation function of hard segment is ~0.4 at DR = 6, not very different from that of soft segment, ~0.3.

Thermal annealing affects this sample quite differently as compared with the other sample, i.e., Esrel 1040M. For soft segments, annealing does not change the orientation

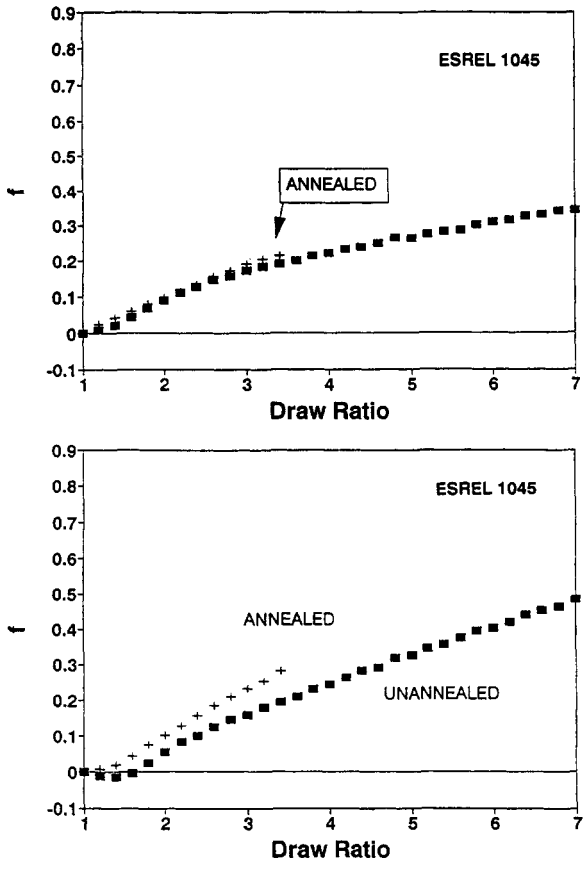

Figure 7. Orientation function of Esrel 1045 as a function of draw ratio: (a, top) C–H stretching (b, bottom) aromatic C–H bending.

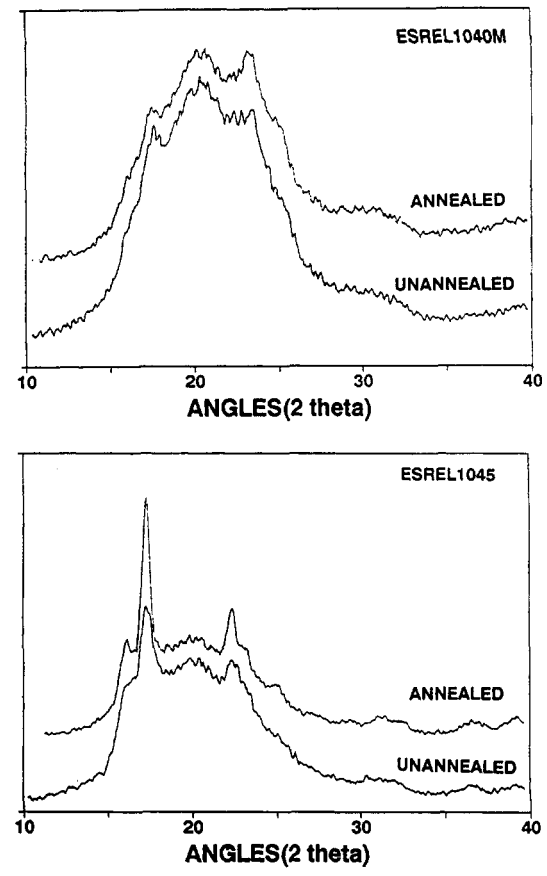

Figure 8. Wide-angle X-ray diffractogram of PBT-co-PTMO before and after annealing at 145 °C for 15 h: (a, top) Esrel 1040M, (b, bottom) Esrel 1045.

function significantly. However, the effect of annealing on the hard segment is not negligible. Compared with annealed Esrel 1040M, which exhibits a noticeable decrease in hard-segment orientation (Figure 6b), annealed Esrel 1045 shows the opposite effect of annealing on the orientation of hard segments. From the results in Figures 6 and 7, it would be natural to assume that two polymers, Esrel 1040M and 1045, have very different molecular structures.

Even though the hard segment contents of the two polymers differ only by ~6%, the degree of phase separation appears to be vastly different. Esrel 1040M polymers contain a small amount of aromatic chain extender in addition to the butanediol. The additional chain extender seems to be enough to break the regularity of the hard segments resulting in the rather lower degree of phase separation and decreased melting temperature. The melting temperature data in Table 1 are consistent with the infrared results.

The negative orientation function at a small degree of deformation has been observed in many cases for a variety of polymers such as polyethylene-,[21-24] and polyester-,[25] nylon-,[26] polyvinyl chloride-,[27] polyurethane,[28,29] and polyester-based block copolymers.[12] Even though an exact explanation has still to be obtained, it is generally accepted that the long axis of the lamellae tends to orient along the deformation direction, resulting in a negative orientation as observed in Figure 7b. Since the lamellae of crystalline structure have been observed through the transmission electron microscope for the polyester-based segmented copolymers,[6] the explanation for the negative orientation observed seems to be appropriate for this copolymer.

The fact that the negative orientation behavior does not exist for the hard segment of Esrel 1040M polymer is consistent with the low degree of phase separation found for this polymer. For the unannealed Esrel 1040M sample, most of the hard segments are dissolved in the soft matrix. These hard segments are easily aligned along with the soft matrix toward the deformation direction. This can result in the very high orientation function of the hard segment (Figure 6b). Since the glass transition of the hard segment is well above the room temperature, the orientation developed remains unchanged.

The major effects of annealing on the copolymer can be changes of the overall crystallinity and degree of phase separation. In Figure 8, the wide-angle X-ray diffractograms of the copolymers are shown. Comparing the results in Figure 8 with the wide-angle X-ray studies in PBT polymers,[30,32] it can be easily concluded that the crystal structure of these copolymers is not well-formed, especially for the Esrel 1040M. Furthermore, annealing appears to have negligible effect on the development of the crystallinity. Thus the effect of annealing on the morphology of the copolymers seems to be mainly the enhancement of the degree of phase separation. The gradual increase in the orientation function associated with soft segments for both samples is easily understood. Furthermore, the negligible effect of annealing on the soft-segment orientation is also expected, because the major change induced by the annealing is the enhancement of the degree of phase separation.

Annealing of Esrel 1040M copolymer appears to increase the amount of lamellar structure of the hard domain even though the degree of phase separation after annealing is still far from complete. Since the hard segments in the lamellar domains tend to orient perpendicular to the deformation direction, the orientation of the hard segment of annealed sample is, upon annealing, expected to be lower

than that of unannealed sample, as shown in Figure 6a.

In the case of unannealed Esrel 1045 polymer (Figure 7b), the small negative orientation of the hard segment at low deformation level appears to indicate that the lamellar type domain structure is well-formed before annealing. Thus the effect of annealing on this polymer, compared with Esrel 1040M polymer, is small as expected. The small increase of orientation function upon annealing is not fully understood at this stage. However, if annealing tends to enhance the formation of macroscopically isotropic hard domain structure, for example, spherulites, the net effect of annealing can be the slight increase of orientation function.

Even though the long direction of lamellar domain tends to align toward the deformation direction at small strain, the lamellar domain will undergo structure rearrangement, eventually resulting in the breakup of lamellae into many smaller ones with corresponding alignment of chains in the domain along the deformation direction. The increased orientation function at high draw ratio seems to support that. However, the lower orientation of the annealed sample, compared with the unannealed sample (Figure 6b), appears to indicate that the breakup and alignment of the hard domain are not complete under the experimental conditions used, i.e. up to DR = 5.5.

The orientation functions of the carbonyl stretching peak are also studied using the transition dipole moment angle in Table 2 (data not shown). Even though the absolute value of orientation function of C=O peak is smaller than that of the aromatic C–H stretching peak, the general shapes are very similar. Since the carbonyl group is expected to be nearly coplanar with the aromatic ring due to the conjugated structure,[30,33] the orientation functions of two infrared peaks should not differ significantly. The apparent difference between two peaks seems to be due to the uncertainty in the transition dipole moment angle (α) of the carbonyl stretching peak. In order to equate the orientation functions of two peaks, α of the carbonyl peak should be about 72° rather than 78°.

On the basis of the forementioned infrared results, the phase-separated morphology of two copolymers can be described as follows: First, the degree of phase separation of unannealed Esrel 1040M polymer is very low, which is the original purpose of using the additional chain extender. The degree of phase separation can be, however, enhanced by the heat treatment. Second, Esrel 1045 polymer has the well-defined hard-domain morphology of the lamellar type before annealing. Therefore, the structural change due to the heat treatment is smaller than that of Esrel 1040M polymer. This was manifested by the negative orientation of the hard segment at low draw ratio.

It is clear that infrared dichroic measurements are useful in monitoring segmental orientation of various functional units, and the results can be closely correlated with the morphological state and structural change by a heat treatment.

2. Polarizing Microscopy. Even though the infrared dichroic method is useful to monitor the orientation of an individual functional group, the overall orientation function cannot be obtained directly. The overall orientation function can be calculated with the birefringence value obtained with the polarizing microscope and eq 6,[18]

$$f = \frac{\Delta n}{\Delta n^\circ} \tag{6}$$

where Δn° is the birefringence of a perfectly oriented sample. Since Δn° is constant for a given sample, the orientation function is linearly proportional to birefringence.

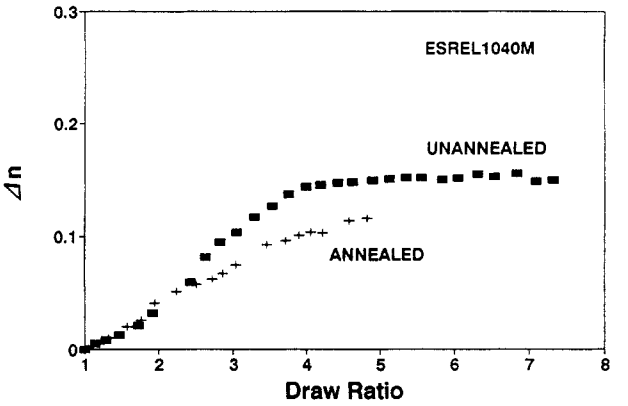

Figure 9. Birefringences of Esrel 1040M as a function of draw ratio. Annealing was done at 145 °C for 15 h.

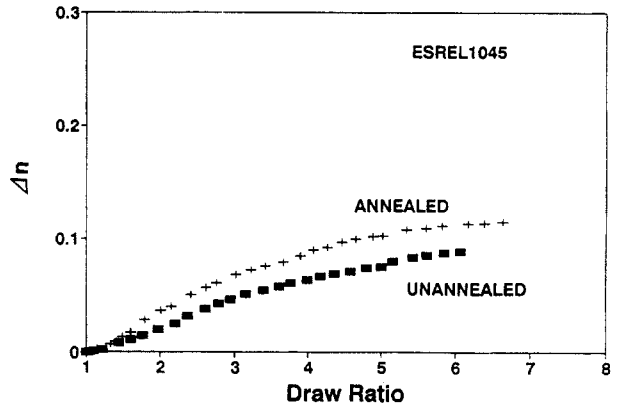

Figure 10. Birefringences of Esrel 1045 as a function of draw ratio. Annealing was done at 175 °C for 15 h.

Birefringence values are shown in Figures 9 and 10 as a function of draw ratio for Esrel 1040M and 1045, respectively. For unannealed Esrel 1040M sample, birefringence increases rapidly with draw ratio up to DR = 4.0 before leveling off. For annealed Esrel 1040M sample, the birefringence was observed to be lower than unannealed sample, especially when the draw ratio is higher than about 2.5. Its value does not seem to level off under the experimental conditions used.

For Esrel 1045 polymer, the birefringence value is smaller than that of Esrel 1040M polymer. Furthermore, annealing of this sample appears to increase the birefringence, which is the opposite effect as compared with Esrel 1040M polymer.

It is generally known that the orientation function calculated from the birefringence value represents the average orientation of all chains in the sample. For the two copolymers used in this study, the weight percent of hard segments is 43.8 (Esrel 1040M) or 50.6 (Esrel 1045). Since there are, as a first-order approximation, similar amounts of hard segments and soft segments in both copolymers, the observed birefringence value may be interpreted as representing an average orientation affected by both segments almost equally.

However, considering the low degree of orientation of soft segments, which constitutes almost 50% (or higher for Esrel 1040M) of copolymer, a birefringence of about 0.15 at DR = 4.0 (and higher) is too high compared with the birefringence value of the polyethylene terephthalate stretched up to DR = 4, which is close to 0.2.[34]

For the unannealed Esrel 1040M sample, the soft-segment-orientation function increased gradually with the

draw ratio, whereas most of the hard-segment orientations developed by DR = 4 (Figure 6). By comparing the two results in Figures 6a and 9 denoted with filled-square data points, it is easily concluded that the birefringence values resemble the orientation behavior of the hard segments far more than that of soft segments. The behavior of decreased birefringence upon annealing also appears to coincide with the hard-segment behavior in Figure 6b. It is to be noted that annealing had the negligible effect on the soft-segment orientation. The strong resemblance between the hard-segment orientation and the orientation behavior obtained with the birefringence may mean that the birefringence value can be preferentially affected by specific structures of chain segments.

The refractive index can be calculated using the Lorenz–Lorentz equation (eq 7),[35,36]

$$n^2 = 1 + \frac{Ne^2}{m\epsilon_0}\sum_j \left(\frac{f_j}{\omega_j^2 - \omega^2}\right) \tag{7}$$

where N is the number of electrons in unit volume, e is the electron charge, m is the electron mass, ϵ_0 is the constant, ω_j is the resonance frequency of the j electron, ω is the frequency of the source electromagnetic wave, and f_j is the mole fraction of j electron. According to Equation 7, all electrons in the polymer chain contribute to the refractive index. However, since each electron may have different resonance frequency, ω_j, the effect of each electron on the refractive index can be very different.

The electrons in the copolymers used in this study can be classified into three types, i.e., σ, nonbonded, and π electrons. Whereas only σ and nonbonded electrons are in the soft segments, hard segments contain π electrons in the aromatic ring and carbonyl group in addition to other types of electrons. It is also to be noted that the π electrons in the hard segmets are conjugated. Generally, the resonance frequency of conjugated electrons is within (or close to) the frequency range of visible light.[36] However, the resonance frequency of σ and nonbonded electrons, compared with conjugated π electrons, is far from visible frequency. Since the refractive index is strongly affected by the electrons, the resonance frequency of which is close to the source frequency (green light for this study), the effect of the hard segments on the refractive index is expected to be much greater than that of soft segments.

For a small birefringence value, the relationship between the birefringence and the chemical structure of the segments can be easily understood using the differentiated Lorenz–Lorentz equation (eq 8),[37]

$$\Delta n = \frac{2\pi}{9}\frac{(\bar{n}^2 + 2)^2}{n}\sum_i \left[(\alpha_1 - \alpha_2)_j \left(\frac{3\langle\cos^2\phi\rangle_j - 1}{2}\right)\right] \tag{8}$$

where $\bar{n}$ is the average value of the refractive indices parallel and perpendicular to the deformation direction. α_1 and α_2 are the polarizability of the segment along and perpendicular to the chain direction, respectively. The term in the last bracket, $((3\langle\cos^2\phi\rangle_j - 1)/2)$, is Herman's orientation function of the j segment.

According to eq 8, the refractive index is affected by the polarizability difference multiplied by the Herman's orientation function of all segments. Since the hard segment contains conjugated structures, i.e., aromatic ring and carbonyl group, its polarizability difference is expected to be significantly greater than that of soft segments. Thus the effect of the hard segment on the refractive index will be larger than that of the soft segment, as observed in Figure 9. Furthermore, the preferential effect of the hard segment is amplified by the higher orientation of the hard segment in Esrel 1040M.

The fact that the orientation determined by the birefringence deviates from the average value of all segments appears to indicate that the birefringence value obtained with the polarizing microscope is preferentially affected by the π electrons of the hard segments. These results mean that the chemical structure of the all constituents has to be considered when the degree of orientation is deduced from the birefringence value of the materials with heterogeneous structure such as thermoplastic elastomers.

Conclusions

The orientational behavior of the polymer chains can be analyzed with the various types of characterization methods. However, infrared dichroic and Raman scattering method are unique to study the orientational behavior of the individual segment separately due to the inherent selectivity of these methods.[20,38-40] This property of these vibrational spectroscopies is very useful in following the orientational behavior of the phase-separated, heterogeneous thermoplastic elastomers.

In this study, the orientational behavior of two thermoplastic elastomers has been observed to be distinctively different even though the chemical structure and the hard-segment contents are quite similar. The annealing effect on the orientation has been also quite different, depending on the phase-separated structure before annealing.

The orientation of the hard segments of the Esrel 1040M sample has been observed to increase rapidly upon stretching, whereas that of the soft segment increased gradually and its magnitude was smaller than that of the hard segment. It is due to the ill-developed phase-separated structure. Since most of the hard segments are dispersed in the amorphous domain, the shear flow of the amorphous domains induces the orientation of the hard segment. Once the hard segments orient, orientation relaxation hardly occurs due to the high glass transition temperature of the hard segments. However, the orientation of the soft segment relaxes rapidly, resulting in the lower orientation due to the lower glass transition temperature of the soft segment.

For the well-phase-separated sample (Esrel 1045), the hard segment orientation was observed to be lower than that of Esrel 1040M. It is attributed to the hard *domain* orientation rather than hard *segment* orientation. The negative orientation of the hard segment at lower draw ratio seems to support that argument. At higher draw ratio, the hard domains breakup, finally resulting in the increased hard-segment orientation as observed experimentally.

By comparing the orientational behavior of the two samples, it can be concluded that two samples have very different morphological states and it is mostly due to the additional small amount of aromatic chain extender which is enough to perturb the crystalline structure of the hard segments.

The variation of the birefringence value as a function of the draw ratio has been observed to resemble the orientation of the *hard* segment far more than that of the *soft* segment. It is interpreted in terms of the different types of electrons in each segments. π electrons in the hard segment appear to affect preferentially the birefringence value. On the basis of the experimental observation, it can be concluded that the interpretation of the orientation with the birefringence value should not be done directly, especially for the copolymers like thermoplastic

elastomers. The chemical structures of each segment and the nature of the electrons in each segment should be considered in order to get the correct orientation behavior from the birefringence.

Acknowledgment. We should like to thank Cheil Synthetic Inc., (Gi-heung, Korea) for supplying the samples. We are also grateful to Dr. S. L. Hsu for reviewing and providing many good suggestions and corrections.

References and Notes

(1) Parris, R. W. "History of Rubber Industry", Schidrowity, P., Dawson, T. R., Eds.; Institution of Rubber Industry, London, 1952.
(2) "Encyclopedia of Polymer Science and Engineering." Kroschwitz, J. I. et al., Eds.; Wiley-Interscience: New York, 1985; Vol. 14, pp 670–804.
(3) Wells, S. C. *Handbook of Thermo-Plastic Elastomers*; Walker, B. Ed.; van Nostrand Reinhold, New York, 1979; Chapter 4.
(4) Goodman, I. Ed. *Developments in Block Copolymers-1*; Applied Science Publishers: Barking, UK, 1982.
(5) Brown, M.; Witsiepe, W. K. *Rubber Age* **1972**, March, 35.
(6) Cella, R. J. *J. Polym. Sci. Polym. Symp.* **1973**, *42*, 727.
(7) Seymour, R. W.; Overton, J. R.; Corley, L. S. *Macromolecules* **1975**, *8*, 331.
(8) Perego, G.; Cesari, M.; Fortuna, G. D. *J. Polym. Sci.* **1984**, *29*, 1141.
(9) Perego, G.; Cesari, M.; Vitali, R. *J. Polym. Sci.* **1984**, *29*, 1157.
(10) Briber, R. M.; Thomas, E. L. *Polymer* **1986**, *27*, 66.
(11) West, J. C.; Lilaonitkul, A.; Cooper, S. L.; Mehra, U.; Shen, M. *ACS Polym. Preprints* **1974**, *15* (2), 191.
(12) Lilaonitkul, A.; West, J. C.; Cooper, S. L. *J. Macromol. Sci. Phys.* **1976**, *B12*, 563.
(13) Shen, M.; Mehra, U.; Niinomi, M.; Koberstein, J. T.; Cooper, S. L. *J. Appl. Phys.* **1974**, *45*, 4182.
(14) Estes, G. M.; Seymour, R. W.; Cooper, S. L. *Macromolecules* **1971**, *4*, 452.
(15) Cunningham, A.; Ward, I. M.; Willis, H. A.; Zichy, V. *Polymer* **1974**, *15*, 749.
(16) Fraser, R. D. B. *J. Chem. Phys.* **1953**, *21*, 1511.
(17) Fraser, R. D. B. *J. Chem. Phys.* **1956**, *24*, 89.
(18) Hemsley, D. A. *Applied Polymer Light Microscopy*, Elsevier Applied Science: London, 1989.
(19) Zbinden, R. *Infrared Spectroscopy of High Polymers*, Academic Press: New York, 1964.
(20) Siesler, H. W.; Holland-Moritz, K. *Infrared and Raman Spectroscopy of Polymers*, Marcel Dekker Inc.: New York, 1980.
(21) Holmes, D. R.; Miller, R. G.; Palmer, R. P.; Bunn, C. W. *Nature* **1953**, *171*, 1104.
(22) Keller, A.; Sandeman, I. *J. Polym. Sci.* **1955**, *15*, 133.
(23) Aggarwal, S. L.; Tilley, G. P.; Sweeting, O. J. *J. Polym. Sci.* **1959**, *1*, 91.
(24) Hoshino, S.; Powers, J.; Lereand, D. J.; Kawai, H.; Stein, R. S. *J. Polym. Sci.* **1962**, *58*, 185.
(25) Quynn, R. G.; Steele, R. *Nature* **1954**, *173*, 1240.
(26) Caroti, G.; Dusenbury, J. H. *J. Polym. Sci.* **1956**, *22*, 399.
(27) Tasumi, M.; Shimanouchi, T. *Spectrochim. Acta* **1961**, *17*, 731.
(28) Lin, S. B.; Hwang, K. S.; Tsay, S. Y.; Cooper, S. L. *Colloid Polym. Sci.* **1985**, *263*, 128.
(29) Seymour, R. W.; Allegrezza, A. E., Jr.; Cooper, S. L. *Macromolecules* **1973**, *6*, 896.
(30) Yokouchi, M.; Sakakibara, Y.; Chatani, Y.; Tadokoro, H.; Tanaka, T.; Koda, K. *Macromolecules* **1976**, *9*, 266.
(31) Stambaugh, B.; Koenig, J. L.; Lando, J. B. *J. Polym. Sci. Phys.* **1979**, *17*, 1053.
(32) Huo, D. P.; Cebe, P.; Capel, M. *J. Polym. Sci. Phys.* **1992**, *30*, 1459.
(33) Stambaugh, B.; Koenig, J. L.; Lando, J. B. *J. Polym. Sci. Phys.* **1979**, *17*, 1053.
(34) Brandrup, J., Immergut, E. H., Eds. *Polymer Handbook*; John Wiley & Sons: New York, 1989.
(35) Fowles, G. R. *Introduction to Modern Optics*, 2nd ed.; Holt Rienhart & Winston Inc.: 1968.
(36) Musikant, S. *Optical Materials* Marcel Dekker Inc.: New York, 1990; Vol. 1.
(37) Ward, I. M. *Structure and Properties of Oriented Polymers* Applied Sci. Pub.: Barkin, UK, 1975.
(38) Bower, D. I. *J. Polym. Sci. Phys.* **1972**, *10*, 2135.
(39) Jasse, B.; Koenig, J. L. *J. Macromol. Sci. Rev. Macromol. Chem.* **1979**, *C17*(1), 61.
(40) Pigeon, M.; Prud'homme, R. E.; Pezolet, M. *Macromolecules* **1991**, *24*, 56.